

Cite this article as: Rare Metal Materials and Engineering, 2019, 48(1): 0001-0008.

ARTICLE

# Influence of Small Indium Addition on Microstructures and Tensile Properties of Al-Cu-1.0Li-(Mg) Alloy

Ma Yunlong<sup>1,2</sup>, Li Jinfeng<sup>1</sup>, Liu Danyang<sup>1</sup>, Zheng Ziqiao<sup>1</sup>

<sup>1</sup> Central South University, Changsha 410083, China; <sup>2</sup> Beijing Institute of Aerospace Systems Engineering, Beijing 100076, China

**Abstract:** The tensile properties, aging precipitate type and distribution in Al-Cu-Li-(0.35Mg)-(0.2In) alloy were investigated. In the T6 aged Al-Cu-Li alloy, the aging precipitates are T1(Al<sub>2</sub>CuLi) and  $\theta'$ (Al<sub>2</sub>Cu). As 0.2%In is added, many square-shaped cubic precipitates Al<sub>5</sub>Cu<sub>6</sub>Li<sub>2</sub> were formed at the early aging stage and their sizes keep stable with the extension of aging time. Meanwhile, the  $\theta'$  precipitation is promoted, therefore the aging response of alloy is accelerated and its strength is enhanced. The combined addition of In + Mg suppresses the precipitation of cubic Al<sub>5</sub>Cu<sub>6</sub>Li<sub>2</sub>, but plays a role in promoting T1 precipitation instead. This role is smaller than that of the combined addition of Ag + Mg in 2050 Al-Cu-Li alloy, which results the strength of the In + Mg micro-alloyed Al-Cu-Li alloy being lower than that of the Ag + Mg micro-alloyed Al-Cu-Li alloy 2050. At T8 temper, the role of both In independent addition and In + Mg combined addition are suppressed by the dislocations introduced by plastic deformation prior to artificial aging.

**Key words:** Al-Cu-Li alloy; tensile property; microstructure; indium addition

Li-containing Al alloys are considered as prospective materials in the aircraft and aerospace industry because of their low density, high specific strength, good toughness and low temperature properties<sup>[1]</sup>. Developing new Al-Li alloys has attracted research interest all of the world.

The most prospective method for developing new Al-Li alloys is to add micro-alloying elements to Al-Cu-Li based alloys. Zr, Mn and Mg are the most commonly used micro-alloying elements. Zr element deters the re-crystallization and grain coarsening of Al-Li alloys by forming Al<sub>3</sub>Zr particles<sup>[2-4]</sup>. Mn addition is beneficial for reducing the heterogeneity of Al-Li alloys<sup>[5]</sup>. Mg addition can promote the nucleation of T1 precipitates and accelerate the aging response of Al-Li alloys<sup>[6,7]</sup>.

It has not been found that the independent addition of Ag plays a big role in ameliorating the precipitate distribution and improving the strength of Al-Li alloys<sup>[8]</sup>. However, after the 1990's, it was reported that combined addition of Ag and Mg powerfully promoted the uniform formation of T1 precipitates, refined their sizes, and therefore greatly enhanced

the strength of Al-Li alloys<sup>[9]</sup>. The representative Al-Li alloys micro-alloyed with Mg+Ag include 2195, 2050 and 2198 alloys. 2195 Al-Li alloy has been successfully applied to the super lightweight tank of the space shuttle<sup>[10]</sup>, while 2050 Al-Li alloy has recently entered the industrial production for various commercial aircrafts as a replacement of 7050 alloy<sup>[11]</sup>. The combined addition of Mg+Zn shows a similar function as the combined addition of Mg and Ag<sup>[12,13]</sup>. The corresponding Mg + Zn micro-alloyed Al-Li alloys include 2099, 2199 and 2A97 alloys.

It was reported that the trace addition of In elements in Al-Cu alloys increases the population density of  $\theta'$  precipitates, accelerates aging response of the alloys and enhances their strength<sup>[14,15]</sup>. Gilmore et al found that ~0.1%In highly accelerated the aging response and enhanced the peak yield strength of Al-4.0Cu-1.2Li alloy aged at 160 °C by increasing the thickness of  $\theta'$  precipitates, but little difference was noted in mechanical properties or micro-structures when ~0.1%In was added to Al-4.3Cu-1.3Li-0.5Mg alloy<sup>[16]</sup>. However, Pan et al<sup>[17,18]</sup> investigated the precipitates of

Received date: August 30, 2018

Foundation item: National High-technology Research and Development Program of China ("863" Program) (2013AA032401)

Corresponding author: Li Jinfeng, Ph. D., Professor, School of Materials Science and Engineering, Central South University, Changsha 410083, P. R. China, E-mail: [lijinfeng@csu.edu.cn](mailto:lijinfeng@csu.edu.cn).

Copyright © 2019, Northwest Institute for Nonferrous Metal Research. Published by Science Press. All rights reserved.

Al-3.5Cu-1.0Li-0.5In and Al-3.3Cu-0.8Li-0.5In alloys aged at 175 °C and found a new cubic precipitate, which was not found in other Al-Cu-Li alloys. In this case, the effect of 0.2%In addition on the tensile properties and microstructure of Al-Cu-Li alloys was investigated. Furthermore, considering that Ag+Mg combined addition plays a powerful role in promoting uniform the formation of T1 precipitates and refining their size, the effect of In + Mg combined addition were therefore studied and compared to the effect of Ag + Mg combined addition on 2050 Al-Li alloy.

## 1 Experiment

Four Al-Cu-Li alloys were casted. Their chemical compositions are shown in Table 1. Alloy 1# and alloy 2# were used to investigate the effect of independent In addition on Al-Cu-Li alloy. Their Cu and Li concentrations were controlled to be 3.4% and 1.0% as far as possible. Because of uncontrollable factors during melting, there are small differences, but it was still valid. Alloy 4# is a nominal 2050 Al-Li alloy, and alloy 3# and alloy 4# were used to investigate the different micro-alloying effects of Ag+Mg and In+Mg combined additions.

After homogenization treatment, the ingots were rolled to sheets with 2 mm thickness through a hot rolling and cold rolling process. The sheets were then subjected to T6 temper and T8 temper after solid solution treatment at 520 °C, and quenching in water at room temperature. The T6 temper was artificially aging at 175 °C. The T8 temper was an artificial aging treatment performed at 155 °C after 6% pre-deformation through cold rolling.

Tensile specimens with a parallel section of 30 mm in length and 8 mm in width were cut from the aged sheets in the rolling direction, according to the national standard GB/T228.1-2010. Tensile tests were carried out in a MTS testing machine (MTS858 Mini Bionix II, USA) at a tensile rate of 2 mm/min. The microstructure was observed through using a TecnaiG<sup>2</sup> 20 ST transmission electron microscopy (TEM). The TEM samples were prepared by a twin-jet electro-polishing device in a solution of 75% methanol and 25% nitric acid at -40~20 °C with a voltage of 15~30 V and a current of 70~95 mA.

## 2 Results

### 2.1 Strength variation caused by small addition of In

Table 1 Chemical compositions of the studied alloys (wt%)

Alloy	Cu	Li	Mg	Ag	In	Mn	Zr	Al
1#	3.44	0.99	-	-	-	0.35	0.12	Bal.
2#	3.35	0.99	-	-	0.2	0.35	0.12	Bal.
3#	3.58	1.00	0.35	-	0.2	0.35	0.12	Bal.
4#	3.59	1.02	0.35	0.35	-	0.35	0.12	Bal.

### 2.1.1 In Al-3.4Cu-1.0Li alloy

Fig.1 shows the tensile strength and yield strength of In-free (alloy 1#) and 0.2%In-containing (alloy 2#) Al-3.4Cu-1.0Li alloys as a function of T6 aging time at 175 °C. It can be seen that the tensile strength and yield strength of the T6 aged Al-3.4Cu-1.0Li alloy containing 0.2%In are greatly enhanced by 0.2%In addition. Meanwhile, the T6 aging response is accelerated by 0.2%In addition, considering that the strength of these two solutionized alloy is similar.

Fig.2 shows the tensile strength and yield strength of In-free (alloy 1#) and 0.2%In-containing (alloy 2#) Al-3.4Cu-1.0Li alloys as a function of T8 aging time at 155 °C. Compare to the strength of T6-aged alloys, the strength of these two T8-aged alloys is improved and the difference in strength is much smaller. However, the strength of T8 aged In-free alloy (alloy 1#) is slightly higher than that of the T8 aged 0.2%In-containing alloy (alloy 2#), which is opposite to that of the T6 aging. The lower strength of T8-aged alloy 2# may be associated with its lower Cu concentration, because the Cu concentration of alloy 2# is about 0.1% lower than that of alloy 1#. Furthermore, the T8 aging responses of these two alloys are similar. The influence of 0.2%In addition on enhancing the strength of T6 aged Al-Cu-Li alloy is suppressed by plastic deformation prior to artificial aging.

### 2.1.2 Comparison of small addition of In and Ag in Al-3.6Cu-1.0Li-0.35Mg alloy

Fig.3 shows the tensile strength and yield strength of 0.2%In-containing (alloy 3#) and 0.4%Ag-containing (alloy 4#) Al-3.6Cu-1.0Li-0.35Mg alloys as a function of T6 aging

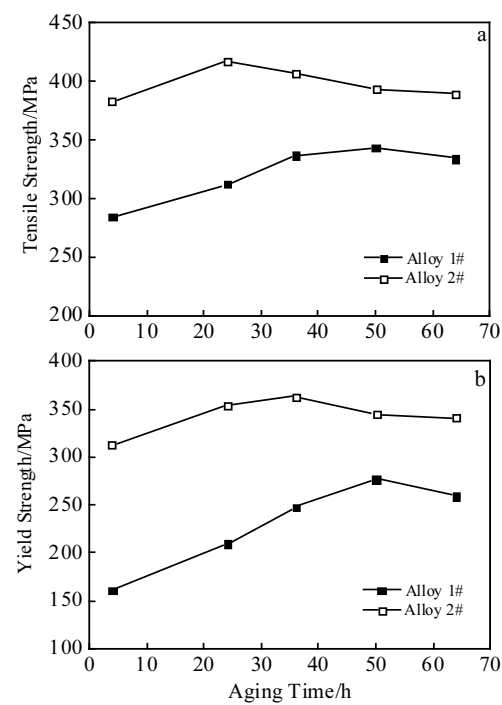


Fig.1 Tensile strength (a) and yield strength (b) of alloys 1# and 2# as a function of T6 aging time at 175 °C

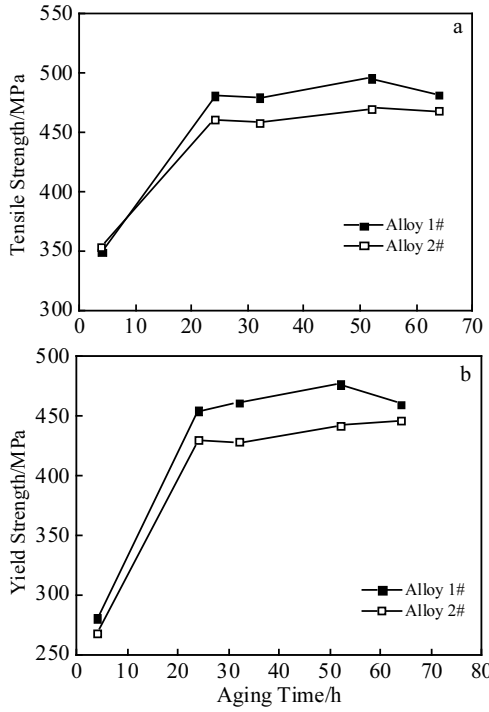


Fig.2 Tensile strength (a) and yield strength (b) of alloys 1# and 2# as a function of T8 aging time at 155 °C

time at 175 °C. The tensile strength of the Ag-containing alloy (alloy 4#) is obviously higher than that of the In-containing alloy (alloy 3#). However, the yield strength of alloy 4# is only a little higher than that of alloy 3#. That is to say, compared to the combined addition of 0.35Mg+0.2In, the combined addition of 0.35Mg+0.35Ag mainly enhances the tensile strength. Due to almost same concentrations of Cu, Li and Mg in alloys 3# and 4#, the strength difference should be associated with different effects of the In and Ag additions or the of In+Mg and Ag+Mg combined additions.

Again, the deformation prior to artificial aging at 155 °C enhances the strength of these two aged alloys (3# and 4#), and diminishes their strength differences (Fig.4). The effects of combined additions of In+Mg and Ag+Mg are lowered by the deformation prior to artificial aging.

## 2.2 Microstructures

### 2.2.1 Effect of 0.2%In addition on precipitates of Al-3.4Cu-1.0Li alloy

Fig.5 shows the TEM bright field (BF) images of alloy 2# containing 0.2%In and alloy 1# without In addition after T6 under-aging at 175 °C for 4 h, which are viewed along  $<100>_{\text{Al}}$  direction. T1 ( $\text{Al}_2\text{CuLi}$ ) precipitates are not found in alloy 2#, there were some  $\theta'$  ( $\text{Al}_2\text{Cu}$ ) precipitates and many square-shaped phases (Fig.5a). Pan et al.<sup>[17,18]</sup> investigated this square-shaped precipitate in detail, and determined that it has a primitive cubic crystal structure with a lattice parameter  $a \approx 0.83$  nm, and the orientation relationship with Al matrix is

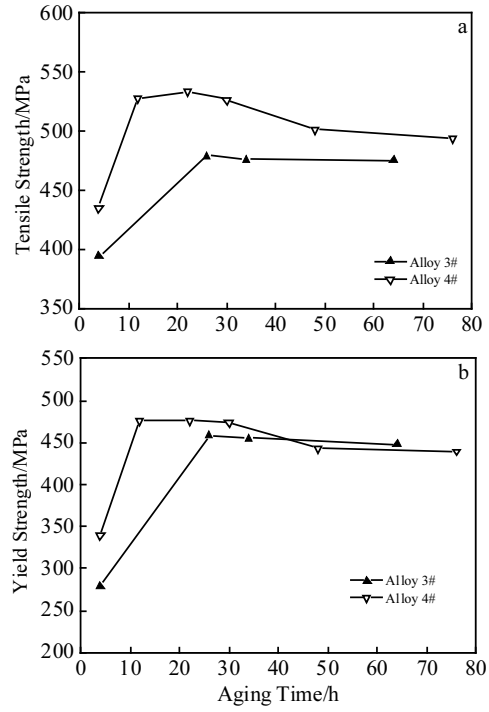


Fig.3 Tensile strength (a) and yield strength (b) of alloys 3# and 4# as a function of T6 aging time at 175 °C

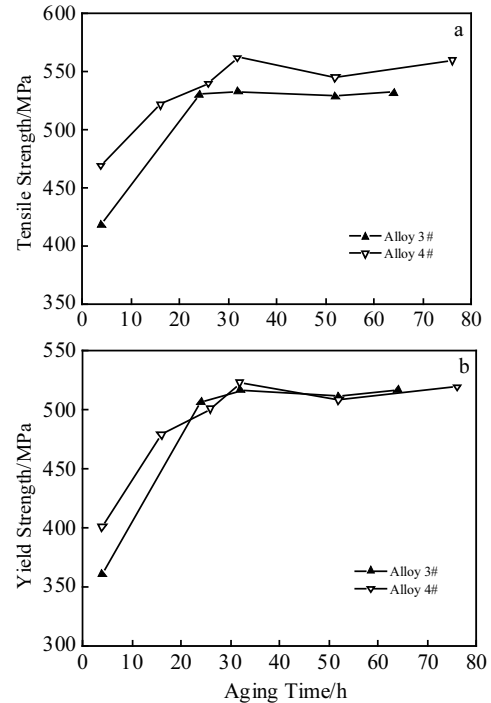


Fig.4 Tensile strength (a) and yield strength (b) of alloys 3# and 4# as a function of T8 aging time at 155 °C

$\{001\}_p/\{001\}_{\text{Al}}, <010>_p//<010>_{\text{Al}}$ , meaning that it is almost coherent with the Al matrix. Meanwhile, no In atom was de-

tected in this square-shaped precipitate and it is assumed as  $\text{Al}_5\text{Cu}_6\text{Li}_2$ , a variant of  $\text{Al}_5\text{Cu}_6\text{Mg}_2$  where Li substituted the Mg positions. For simplicity, this cubic phase is referred to  $\chi$  phase. However, in the alloy 1#, it is difficult to find any precipitates (Fig.5b). This above microstructure features indicate that in the Mg-free Al-3.4Cu-1.0Li alloy, the addition of 0.2%In accelerates the precipitation of  $\theta'$  and results in forming a cubic precipitate  $\chi$  ( $\text{Al}_5\text{Cu}_6\text{Li}_2$ ) at the early aging stage.

Fig.6 shows the TEM images of alloy 2# containing 0.2%In and alloy 1# without In addition after T6 peak aging. Compared to the under-aged alloy, the number density of cubic  $\chi$  precipitates in the peak-aged alloy 2# is greatly increased, and that of  $\theta'$  precipitates is also slightly increased a little. It is of interest that the size of the cubic  $\chi$  precipitates is not enlarged obviously (Fig.6a). Meanwhile, some T1 precipitates are observed in the dark field (DF) image viewed along  $\langle 112 \rangle_{\text{Al}}$  direction (Fig.6b). In the In-free alloy 1#,  $\theta'$  precipitates (Fig.6c) and T1 precipitates (Fig.6d) are observed, but their size is much larger than that of the alloy 2#.

Fig.7 shows the TEM images of the T8 peak-aged alloy 1# and alloy 2#. Compared to the T6 aged alloys, some features

are observed. First, in the T8 peak-aged alloy 2# containing 0.2% In, the cubic  $\chi$  precipitates disappear. Second, in both alloy 1# and alloy 2#, the precipitates are  $\theta'$  and T1, and their number density is increased a lot. In addition, it seems that the T1 number density in alloy 2# is a little smaller, due to its lower Cu concentration.

According to the above TEM observations, the effects of 0.2%In addition on the microstructures of Mg-free Al-3.4Cu-1.0Li alloy are as follows: (1) At T6 aging, it results in the formation of a large number of square-shaped cubic precipitates  $\text{Al}_5\text{Cu}_6\text{Li}_2$ . (2) At T6 aging, it accelerates the precipitation of  $\theta'$ . (3) At T8 aging, the above effects caused by 0.2%In addition are suppressed by plastic deformation prior to artificial aging, which accelerates the uniform and concentrated precipitation of T1.

## 2.2.2 Microstructures of Al-3.6 Cu-1.0Li-0.35Mg alloys containing 0.2%In or Ag

The effect of In+Mg combined addition is different from that of In independent addition. Fig.8 shows the TEM images of T6 under-aged and peak-aged alloy 3# containing 0.2%In and 0.35%Mg simultaneously. As aged for 4 h, only a very small number of cubic precipitates  $\chi$  and GP zones are observed

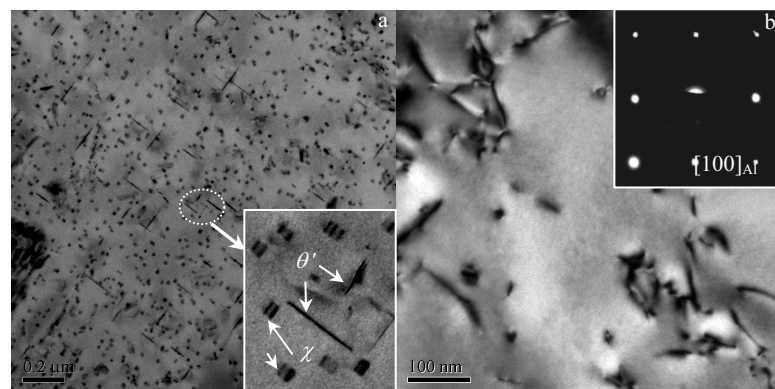


Fig.5 TEM BF images of the alloy 2# (a) and 1# (b) after T6 aging at 175 °C for 4 h (0.2%In-containing alloy showing  $\theta'$  and  $\chi$  precipitates, the direction is parallel to  $\langle 100 \rangle_{\text{Al}}$ )

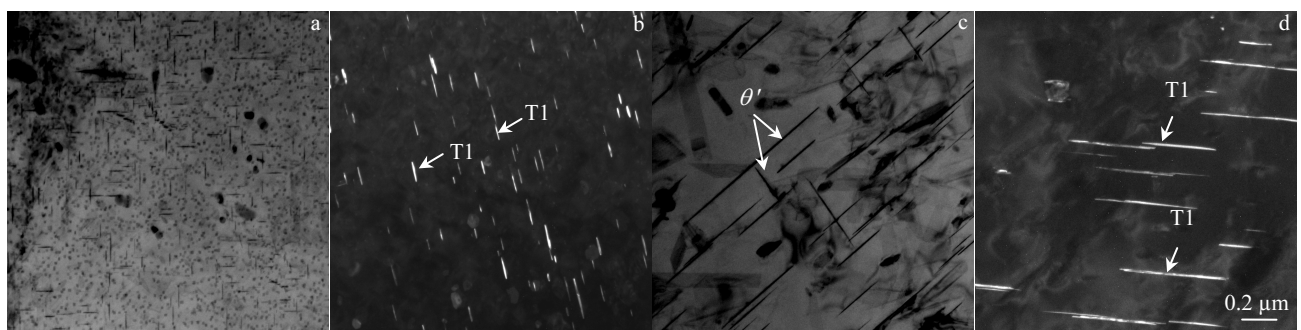


Fig.6 TEM images of the T6 peak-aged alloys: (a) alloy 2# BF image showing  $\theta'$  and  $\chi$  precipitates, the direction is parallel to  $\langle 100 \rangle_{\text{Al}}$ ; (b) alloy 2# DF image showing T1 precipitates, the direction is parallel to  $\langle 112 \rangle_{\text{Al}}$ ; (c) alloy 1# BF image showing  $\theta'$  precipitates, the direction is parallel to  $\langle 100 \rangle_{\text{Al}}$ ; (d) alloy 1# DF image showing T1 precipitates, the direction is parallel to  $\langle 112 \rangle_{\text{Al}}$

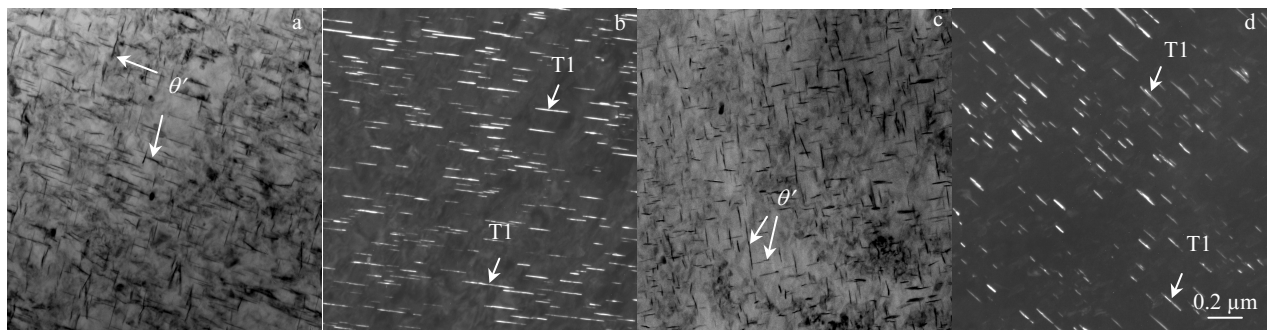


Fig.7 TEM images of the T8 peak-aged alloys: (a) alloy 1# BF image showing  $\theta'$  precipitates, the direction is parallel to  $<100>_{\text{Al}}$ ; (b) alloy 1# DF image showing T1 precipitates, the direction is parallel to  $<112>_{\text{Al}}$ ; (c) alloy 2# BF image showing  $\theta'$  precipitates, the direction is parallel to  $<100>_{\text{Al}}$ ; (d) alloy 2# DF image showing T1 precipitates, the direction is parallel to  $<112>_{\text{Al}}$

(Fig.8a), but a considerable amount of T1 phase is precipitated (Fig.8b). In the peak-aged alloy, the main precipitates are  $\theta'$  and T1 (Fig.8c, 8d), and the population density and size of T1 precipitates are increased (Fig.8d) compared to those in the alloy under-aged for 4 h. It is noted that there are some cubic precipitates  $\chi$  (Fig.8c). The role of In independent addition in forming cubic  $\chi$  precipitates and accelerating  $\theta'$  precipitation is weakened by In+Mg combined addition, which accelerates T1 precipitation instead.

Fig.9 shows the SAED (selected area electron diffraction) patterns and TEM DF images of T6 peak-aged alloy 4# micro-alloyed with Ag + Mg. No cubic precipitates are found. Compared to that in alloy 3# micro-alloyed with In + Mg, it seems that the number density of T1 precipitates in alloy 4# is increased, but their diameter is a little decreased (Fig.9b). Meanwhile, it seems that the number density and diameter of  $\theta'$  precipitates are a little increased (Fig.9a). Combined Ag + Mg addition plays a bigger role in promoting T1 nucleation and precipitation.

Fig.10 shows TEM images of T8 peak-aged alloy 3# micro-alloyed with In+Mg and alloy 4# micro-alloyed with Ag+Mg. Both T8 aged alloys possess similar microstructures, and their aging precipitates are  $\theta'$  and T1. Meanwhile, T1 population density in the T8 aged alloy is much higher, but their size

is much smaller than that in the corresponding T6 aged alloy.

### 3 Discussion

#### 3.1 Effect of 0.2%In independent addition in Al-Cu-Li alloy at T6 aging

0.2%In independent addition causes the formation of cubic  $\chi$  phases, accelerates  $\theta'$  precipitation, and retards T1 precipitation at T6 aging. The most important effect caused by 0.2%In independent addition in Al-Cu-Li alloy in this case is the formation of a large number of cubic phases  $\chi$ , which are In-free and possess a much small strain energy compared with the Al matrix [17,18]. Furthermore, it is difficult for these cubic phases  $\chi$  to coarsen as the aging time is extended (Fig.5a, Fig.6a), which means their very low interfacial energy. Compared to  $\chi$  phase, T1 precipitate is semi-coherent with the matrix and possesses a higher strain energy and interfacial energy. It is known that during solid state transformation, in addition to the driving force for nucleation (change in volume-free energy,  $\Delta G_v$ ), there is also energy barrier for nucleation. For a given local super-saturation at a given site, the energy barrier is dependent on the misfit strain energy and interfacial energy. Therefore, the energy barrier for T1 homogeneous nucleation is higher than that for the homogeneous nucleation of cubic  $\chi$  phase.

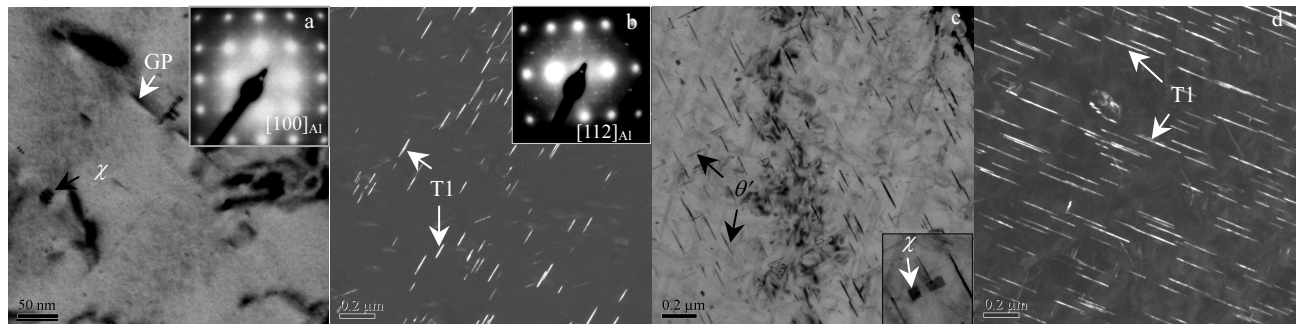


Fig.8 TEM images of alloy 3#: (a, b) T6 under-aging for 4 h, BF image showing  $\chi$  and GP zone, the direction is parallel to  $<100>_{\text{Al}}$ ; (b) T6 under-aging for 4 h, DF image showing T1, the direction is parallel to  $<112>_{\text{Al}}$ ; (c) T6 peak-aging, BF image showing  $\theta'$  and  $\chi$  precipitates, the direction is parallel to  $<100>_{\text{Al}}$ ; (d) T6 peak-aging, DF image showing T1 precipitates, the direction is parallel to  $<112>_{\text{Al}}$

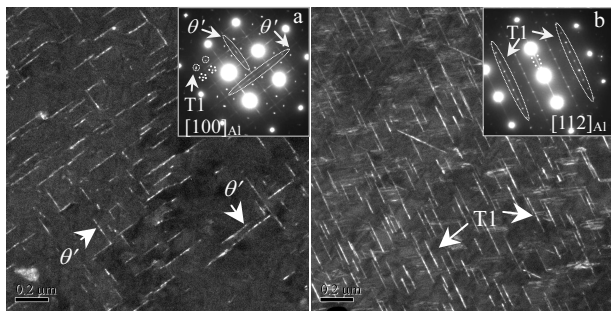


Fig.9 TEM DF images and SAED patterns of T6 peak-aged alloy 4#: (a) showing  $\theta'$  precipitates, the direction is parallel to  $<100>_{\text{Al}}$ ; (b) showing T1 precipitates, the direction is parallel to  $<112>_{\text{Al}}$

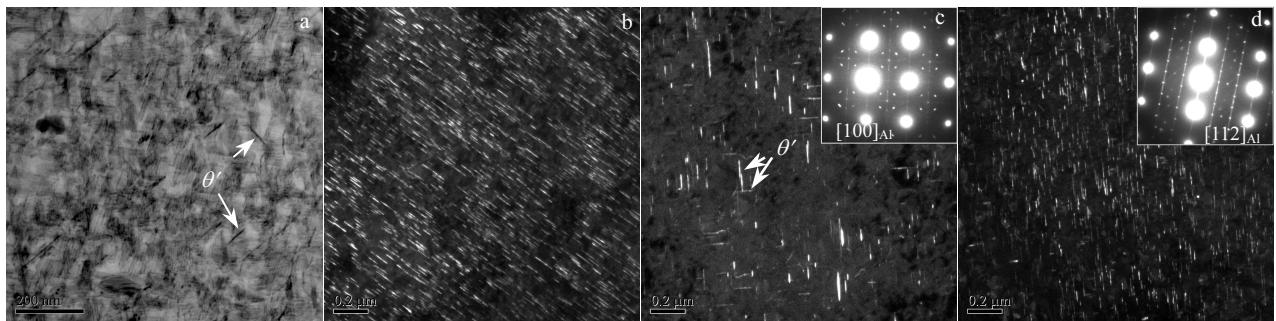


Fig.10 TEM images of T8 peak-aged alloy 3# micro-alloyed with In+Mg (a, b) and alloy 4# micro-alloyed with Ag+Mg (c, d): (a) alloy 3# BF image showing  $\theta'$  precipitates, the direction is parallel to  $<100>_{\text{Al}}$ ; (b) alloy 3# DF image showing T1 precipitates, the direction is parallel to  $<112>_{\text{Al}}$ ; (c) alloy 4# BF image showing  $\theta'$  precipitates, the direction is parallel to  $<100>_{\text{Al}}$ ; (d) alloy 4# DF image showing T1 precipitates, the direction is parallel to  $<112>_{\text{Al}}$

dislocation loops caused by vacancy collapsing, which in turn is not beneficial to the heterogeneous nucleation of T1 precipitates. However, due to the low interfacial energy and small strain energy of  $\chi$  phase, the energy barrier for homogeneous nucleation of  $\chi$  phase is much small. Assuming the similar driving force for T1 and  $\chi$  precipitation, the homogeneous nucleation for  $\chi$  is certainly easier than that for T1 as 0.2%In is added.

As for the mechanism by which In element accelerates  $\theta'$  precipitation, most researchers thought that In-Cu-vacancy clusters were formed during quenching process, which grew and acted as nucleation sites and accelerated  $\theta'$  precipitation [21,22]. Furthermore, Silcock et al [23] proposed that at an aging temperature lower than 200  $^{\circ}\text{C}$ , In-vacancy formed and transported to the interface between the  $\theta'$  precipitate and the Al matrix, and thus decreased the strain energy. The decreased strain energy means a lower energy barrier for  $\theta'$  nucleation, so the nucleation of  $\theta'$  precipitates is therefore accelerated. It is because of the concentrated precipitation of  $\chi$  and  $\theta'$  phases that the strength of the Al-Cu-Li alloy with 0.2%In independent addition is higher than that of the In-free alloy.

For the nucleation, it is necessary to overcome or minimize the energy barrier. Therefore, T1 precipitates prefer to nucleate at the sites of dislocation, interface with low-angle grain boundary, stacking faults and Mg-Cu-vacancy co-cluster, which decrease the barrier energy for nucleation [19].

Considering that T1 precipitation is accelerated and  $\chi$  precipitation is deterred at T8 aging, it is explicit that there is a competitive model between  $\chi$  and T1 nucleation. This competition is associated with its beneficial nucleation sites. After quenching, there are considerable vacancies in Al-Cu-Li alloy which can collapse to form dislocation loops and then act as the heterogeneous nucleation sites for T1 precipitates. As 0.2%In is added, due to the high binding energy between In atoms and vacancy (Fig.11)<sup>[20]</sup>, In-vacancy clusters is formed to trap the vacancies and therefore deters the formation of

### 3.2 Effect of combined addition of In+Mg in Al-Cu-Li alloy at T6 aging

At T6 aging, the role of In independent addition in causing the formation of cubic  $\chi$  precipitates is weakened or suppressed by the In+Mg combined addition, which promotes the uniform and concentrated precipitation of T1 phases instead.

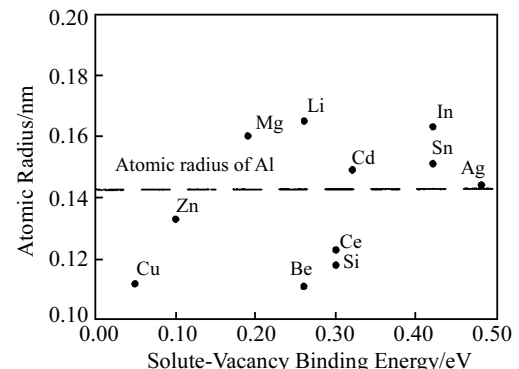


Fig.11 Atomic radius of Al and various solutes as a function of solute vacancy binding energy<sup>[20]</sup>

**Table 2** Calculated enthalpy ( $\Delta H^0$ ) of solution at infinite dilution (kJ/mol)<sup>[24]</sup>

Solute	Solvent					
	Al	Li	Cu	Mg	Ag	In
Al		-15	-34	-7	-17	24
Li	-13		-19	-1	-55	-41
Cu	-28	-18		-15	8	8
Mg	-8	-1	-20		-42	-14
Ag	-18	-65	10	-40		-5
In	31	-59	12	-16	-7	

It is known that Al possesses a higher stacking fault energy, but Mg elements can assemble on the close-packed surface of  $\{111\}_{\text{Al}}$  to decrease the stacking fault energy<sup>[6,7]</sup>. Therefore, as a small amount of Mg is added to Al-Cu-Li alloy, considerable stacking faults are formed. These stacking faults provide beneficial sites for T1 heterogeneous nucleation, because the energy barrier for T1 nucleation is lowered at the stacking faults. Besides, there exists strong interaction between Mg and In, between Li and In, and between Mg and Cu, as predicted by the calculated enthalpies of solution at infinite dilution,  $\Delta H^0$ . Table 2 shows some extracted values of  $\Delta H^0$  from the lists reported by Niessen et al<sup>[24]</sup>. In the solutionized alloy, Mg and In atoms assemble on the close-packed surface of  $\{111\}_{\text{Al}}$ , forming Mg-In atom co-clusters due to their strong interaction. Then, at the early aging stage, Li atoms and Cu atoms are attracted to Mg-In atom co-clusters, due to strong interaction between Li and In atoms and between Cu and Mg atoms. That is to say, as small Mg and In are simultaneously added, the formed stacking faults assembled with Mg atoms provide the sites for T1 heterogeneous nucleation, and Mg-In atom co-clusters act as catalysis and bridge for promoting the diffusion of Cu and Li atoms to the stacking faults. Therefore, the precipitation of T1 is significantly promoted, but that of the  $\chi$  phase is suppressed. Because the strengthening effect of T1 phase precipitated at  $\{111\}_{\text{Al}}$  plane is higher than that of other phases<sup>[25]</sup>, the strength of the Al-Cu-Li alloy with In+Mg combined addition is correspondingly enhanced, compared to that of the alloy with In independent addition.

The role of In+Mg combined addition in promoting the uniform and concentrated precipitation of T1 phases is similar, but is not as much as that of Ag+Mg combined addition. This should be attributed to the interaction difference. As shown in Table 2, the interaction between Mg and In is much smaller than that between Mg and Ag, and the interaction between In and Li is also a little lower than that between Ag and Li. Therefore, the strength of the Al-Cu-Li alloy with In+Mg combined addition is lower than that of the alloy with Ag+Mg combined addition.

It is noted that compared to that of the alloy with combined addition of Ag+Mg (alloy 4#), the yield strength of the alloy with the combined addition of In+Mg (alloy 3#) is much lower, but the tensile strength is only a slightly lower (Fig.3). This is associated with the precipitate types and distribution. In the alloy 3#,

there are some cubic  $\chi$  precipitates, which are coherent, and cause a smaller strengthening effect on the yield strength by dislocation cutting than the semi-coherent T1 and  $\theta'$  precipitates by dislocation bypassing<sup>[26]</sup>. In addition, although the number density of T1 precipitates in the alloy 3# is a little lower (Fig.8a), the diameter is a little increased. This factor contributes to reduce the difference in the tensile strength of alloy 3# and alloy 4#<sup>[27]</sup>.

### 3.3 Role of pre-deformation in suppressing the effect of micro-alloying elements

For the alloys micro-alloyed with independent In and combined In+Mg, the pre-deformation plays a role in suppressing the formation of cubic  $\chi$  phases and promoting uniform and concentrated precipitation of T1. This effect is associated with the dislocations introduced by plastic deformation prior to artificial aging.

As mentioned above, there is a competitive model in the nucleation of T1 and cubic  $\chi$  phases. In the T6 aged Al-Cu-Li alloy micro-alloyed with independent In, the In-vacancy clusters deter the formation of dislocation loops, which is the beneficial sites for T1 precipitation within grains. Therefore, the precipitation of T1 within grains mainly depends on the homogeneous nucleation. But because of its smaller energy barrier for homogeneous nucleation, the cubic phase  $\chi$  wins in the competition of homogeneous nucleation.

However, once the dislocations are introduced through plastic deformation prior to artificial aging, they act as heterogeneous nucleation sites for the precipitates with semi-coherency features (or certain misfit strain energy and interfacial energy), because the dislocations decrease the energy barrier for nucleation. In Al-Cu-Li alloys, these precipitates mainly include T1 and  $\theta'$ . The nucleation rate of T1 and  $\theta'$  is thus enhanced by the pre-deformation. Furthermore, T1 is an equilibrium phase and  $\theta'$  is a metastable phase, and the change in volume-free energy ( $\Delta G_v$ ) associated with T1 precipitation may be larger than in  $\Delta G_v$  associated with  $\theta'$  precipitation. Besides, the shear strain associated with  $\theta'$  on the  $\{001\}_{\text{Al}}$  plane in the  $[100]_{\text{Al}}$  direction is lower than that associated with T1 on the  $\{111\}_{\text{Al}}$  plane in the  $[112]_{\text{Al}}$  direction<sup>[28]</sup>. The above two factors, i.e. the larger  $\Delta G_v$  and the  $\{111\}_{\text{Al}}$  shear strain aid in the heterogeneous nucleation of T1 precipitates on dislocations over that of  $\theta'$  precipitates<sup>[28]</sup>. For the above reasons, the formation of cubic phase  $\chi$  is suppressed, while the precipitation of T1 is accelerated by T8 aging. Consequently, the strength is enhanced and the strength difference between the In-free alloy and In-containing alloy is decreased.

In the Al-Cu-Li alloys micro-alloyed with In+Mg and Ag+Mg, the dislocations introduced by pre-deformation also provide more nucleation sites for T1 precipitation, which results in more concentrated T1 precipitates.

## 4 Conclusions

- 1) In the Al-Cu-Li alloy, 0.2%In independent addition leads to the formation of a large number of square-shaped cubic precipitates  $\text{Al}_5\text{Cu}_6\text{Li}_2$  and promotes the precipitation of  $\theta'$

phases at T6 aging, so the aging response is therefore accelerated and the aging strength is enhanced.

2) The combined addition of In+Mg in Al-Cu-Li alloy inhibits the formation of the cubic precipitates, but promotes the precipitation of T1 at T6 aging. The role of small In independent addition in forming cubic precipitates is suppressed or weakened by small Mg addition.

3) At T6 aging, the combined addition of In+Mg promotes T1 precipitation, but this role is smaller than that of the combined addition of Ag+Mg in 2050 Al-Li alloy, which causes a smaller strength of In- and Mg-containing alloy.

4) At T8 aging, for the Al-Cu-Li alloy with In independent addition, the pre-deformation plays a role in suppressing the formation of the cubic phase and in promoting uniform and concentrated precipitation of T1, which enhances the strength and decreases the strength difference between the In-free alloy and In-containing alloy.

## References

- 1 Rioja R J, Liu J. *Metallurgical and Materials Transactions A*[J], 2012, 43(9): 3325
- 2 Jata K V, Vasudevan A K. *Materials Science and Engineering A*[J], 1998, 241: 104
- 3 Tsivoulas D, Prangnell P B. *Metallurgical and Materials Transactions A*[J], 2014, 45(3): 1338
- 4 Tsivoulas D, Prangnell P B. *Acta Materialia* [J], 2014, 77: 1
- 5 Yang S J, Dai S L, Su B et al. *Transactions of Nonferrous Metals Society of China*[J], 2004, 14(2): 321
- 6 Yi Hongkun, Zheng Ziqiao. *Journal of Central South University of Technology*[J], 1999, 30(3): 292 (in Chinese)
- 7 Gumbmann E, Geuser F De, Deschamps A, et al. *Scripta Materialia*[J], 2016, 110: 44
- 8 Wang Ruiqin, Zheng Ziqiao, Chen Yuanyuan et al. *Rare Metal Materials and Engineering* [J], 2009, 38(4): 622 (in Chinese)
- 9 Huang B P, Zheng Z Q. *Acta Materialia*[J], 1998, 46(12): 4381
- 10 Troeger L P, Wanger J A. *Journal of Materials Processing & Manufacturing Science*[J], 2001, 9(3): 205
- 11 Lequeu P, Smith K P, Danielou A. *Journal of Materials Engineering and Performance*[J], 2010, 19(6): 841
- 12 Luo Xianfu, Zheng Ziqiao, Zhong Jifa et al. *The Chinese Journal of Non-ferrous Metals*[J], 2013, 23(7): 1833 (in Chinese)
- 13 Li J F, Xu L, Cai C et al. *Metallurgical and Materials Transaction A*[J], 2014, 45(12): 5736
- 14 Shu Jun, Chen Zhiguo, Li Shichen et al. *The Chinese Journal of Nonferrous Metals*[J], 2012, 22(9): 2486 (in Chinese)
- 15 Pan Zhengrong, Zheng Ziqiao, Li Shichen et al. *Rare Metal Materials and Engineering* [J], 2011, 40(6): 1079 (in Chinese)
- 16 Gilmore D L, Jr. Starker E A. *Metallurgical and Materials Transactions A*[J], 1997, 28(7): 1399
- 17 Pan Z R, Zheng Z Q, Liao Z Q et al. *Acta Metallurgica Sinica*[J], 2010, 23(4): 285
- 18 Pan Z R, Zheng Z Q, Liao Z Q et al. *Materials Letters*[J], 2010, 64: 942
- 19 Li J F, Ye Z H, Liu D Y et al. *Acta Metallurgica Sinica*[J], 2017, 30(2): 133
- 20 Nie J F, Muddle B C, Aaronsen H I et al. *Metallurgical and Materials Transactions A*[J], 2002, 33(6): 1649
- 21 Hewitt P, Butler E P. *Acta Metallurgica*[J], 1986, 34(7): 1163
- 22 Kimura H, Hasigui R R. *Acta Metallurgica*[J], 1961, 9(12): 1076
- 23 Slickock J M, Flower H M. *Scripta Materialia*[J], 2002, 46: 389
- 24 Niessen A K, de Boer F R, Boom R et al. *Calphad*[J], 1983, 7(1): 51
- 25 Nie J F, Muddle B C. *Materials Science and Engineering A*[J], 2001, 319-321(S1): 448
- 26 Lin Xiaohong, Li Jinfeng, Chen Yonglai et al. *Chinese Journal of Rare Metals* [J], 2017, 41(12): 1293 (in Chinese)
- 27 Nie J F, Muddle B C, Polmear I J. *Materials Science Forum*[J], 1996, 1217-222: 1257
- 28 Gable B M, Zhu A W, Csontos A A et al. *Journal of Light Metals* [J], 2001, 1(1): 1

## 微量 In 对 Al-Cu-1.0Li-(Mg)合金微观组织与拉伸性能的影响

马云龙<sup>1,2</sup>, 李劲风<sup>1</sup>, 刘丹阳<sup>1</sup>, 郑子樵<sup>1</sup>

(1. 中南大学, 湖南 长沙 410083)

(2. 北京宇航系统工程研究所, 北京 100076)

**摘要:** 研究了Al-Cu-Li-(0.35Mg)-(0.2In)合金的拉伸性能、时效析出相类型及其分布。T6峰时效时, Al-Cu-Li合金的时效析出相为T1(Al<sub>2</sub>CuLi)和θ' (Al<sub>2</sub>Cu)相。添加0.2%In时, T6态时效早期形成许多方块状的立方相Al<sub>5</sub>Cu<sub>6</sub>Li<sub>2</sub>, 且随时间延长其尺寸保持稳定; 同时, 可促进θ'相析出, 相应合金的时效响应加速, 强度提高。同时添加In和Mg可抑制Al<sub>5</sub>Cu<sub>6</sub>Li<sub>2</sub>相析出, 但促进T1相析出。In和Mg的复合微合金化效果小于2050铝锂合金中Ag和Mg的复合微合金化效果, 因而In+Mg复合微合金化铝锂合金T6态强度低于Ag+Mg复合微合金化的2050铝锂合金。T8态时效时, 时效前预变形产生的位错抑制了In元素单独添加和In+Mg复合添加的微合金化效果。

**关键词:** 铝锂合金; 拉伸性能; 微观组织; 微量 In 添加

作者简介: 马云龙, 男, 1983年生, 博士, 中南大学材料科学与工程学院, 湖南 长沙 410083, 电话: 010-68382013, E-mail: i56567@sina.com